

# Band Correction of Multispectral Camera

Kevin McKenzie, Thomas Watson, and Dr. Eddie Jacobs

University of Memphis, 3720 Alumni Ave, Memphis, TN 38152

## ABSTRACT

The Survey3 by MAPIR is a multispectral camera that can be mounted to a drone to collect imagery that when processed can give insights into the wellbeing of crops. The Survey3 offers several triple-band filter options, but the most popular is the Red-Green-Near Infrared (RGN) filter which allows agriculturalists to map various vegetation indices like the NDVI. The NDVI index is obtained by computing the difference between Red and Near Infrared (NIR) bands and dividing by the sum of the Red and NIR. Obtaining accurate NDVI values requires that each RGN band be isolated from the other to achieve accurate ratios when applying a vegetation index. If there is leakage in any of the bands, the index results can be misleading. We have found that the Survey3's RGN bands have significant overlap, especially in the NIR band, and the calibration performed in their software is inadequate to resolve this discrepancy. In this paper, we characterize the amount of overlap in the bands and use this information to develop methods for correcting the results. Using a monochromator and calibrated hyperspectral camera for reference, we develop a mathematical model to calibrate the data and compare it with data obtained under similar conditions with the calibrated hyperspectral camera.

**Keywords:** Survey3, multispectral camera, drone, NDVI, vegetation indices, Red-Green-Near Infrared (RGN) filter, band overlap, calibration

## 1. INTRODUCTION

In precision agriculture, remote sensing technology is widely used to monitor crop health and growth.<sup>1</sup> One of the commonly used remote sensing technologies is the use of Red-Green-NIR (RGN) cameras. The MAPIR camera is one such RGN camera that has gained popularity among farmers and researchers due to its affordability and ease of use. However, there are concerns about the accuracy of the MAPIR camera's spectral response and its ability to capture the appropriate wavelengths of light for precise vegetation analysis.

In this paper, we aimed to investigate the spectral response of the MAPIR camera and to develop a correction method to improve its accuracy for vegetation analysis. We conducted a field test in Tucson, Arizona, where we collected images of vegetation using the DJI Mavic Pro Survey3 Bundle purchased from MAPIR. The Survey3 images were processed using our own pipeline, and the results were compared with those obtained from a calibrated hyperspectral camera.

Our investigation into the spectral response of the MAPIR camera involved computing a correction matrix from integration values and finding its radiance calibration using a calibrated hyperspectral sensor. We also compared the Arizona images captured by the MAPIR camera with those captured by the hyperspectral sensor for comparison. The corrected and calibrated version of the images were then obtained using the developed correction method.

The findings of this study are important for farmers and researchers who rely on remote sensing technologies for vegetation analysis. The correction method developed in this study can improve the accuracy of the MAPIR camera and enhance its usefulness in precision agriculture.

---

Further author information: (Send correspondence to Eddie Jacobs)

Kevin McKenzie: kmcknze1@memphis.edu

Thomas Watson: tpwatson@memphis.edu

Eddie Jacobs: eljacobs@memphis.edu, Telephone: (901) 678-2000

## 2. EXPERIMENT METHODOLOGY

This section outlines the methodology used to achieve the objectives of the experiment, which aimed to verify the accuracy of the monochromator and obtain correction matrix for the MAPIR camera. The equipment used, including the monochromator and hyperspectral camera, is described, as well as how they were set up and calibrated. The data acquisition process and the steps taken to ensure measurement accuracy are also discussed. Finally, the creation of the correction matrix and obtaining radiance calibration are explained in detail.

To see the MAPIR camera's spectral response, an experiment was conducted using a monochromator that emits light at a specific wavelength. Images were taken across the camera's wavelength range and counts detected for each wavelength were recorded and plotted on a graph. A monochromator from the Jarrell-Ash Company (Model 82-410)<sup>2</sup> was found in our Electro Optics Lab and used for the experiment. This monochromator uses a tungsten halogen bulb and a diffraction grating that is rotated to adjust the wavelength of the emitted light. An initial experiment was conducted with a Resonon Pika L hyperspectral sensor<sup>3</sup> to ensure the accuracy of the monochromator. The sensor operates in the VNIR range, has 281 bands covering the 400-1000nm wavelength range, and includes additional bands beyond this range. The monochromator emitted wavelengths with variations of only 5-8nms. A wavelength correction table was created based on this experiment and used in all subsequent experiments with the monochromator.

Spectral response was analyzed from both RAW and JPG images in Python. The imageio.v3 library<sup>4</sup> was used in combination with the iio.imread() function<sup>5</sup> to open the JPG files. However, interpreting the data from the RAW files required knowledge of the Bayer sensor of the MAPIR camera. The Bayer sensor captures intensity values in each pixel using a pattern of red, green, and blue filters arranged in a 2x2 matrix per pixel. To reconstruct the full-color image, missing color values are interpolated using neighboring pixels through demosaicing.<sup>6</sup> A custom function was created to debayer the data and convert it to a 3D matrix format with each dimension representing a specific band. Next, a graph was generated to illustrate how the camera responds to the spectral range of light emitted from the monochromator spanning from 500 to 900nm. The spectral response was determined by averaging the intensity values from approximately 1600 pixels within the region capturing the light from the monochromator.

In each pixel, the sensor detects counts based on the amount of light in a scene, which can be subject to distortion due to sensor imperfections.<sup>7</sup> The distortion is calculated by integrating the wavelength of the response curves for each band. A 3x3 matrix describes the distortion element of a pixel in the image, with each row representing the amount of red, green, and NIR in each band and each column representing the RGN bands. Ideally, the spectral response matrix should indicate a 100 percent contribution from red, green, and NIR in the corresponding bands, represented by [1,0,0], [0,1,0], [0,0,1]. The integration values required for the calculation are obtained using the np.trapz() function from NumPy. To generate the correction matrix, the distortion matrix is inverted. Once the correction matrix is obtained, it is multiplied by the RGN counts detected in a pixel to correct for any distortion, resulting in an accurate spectral response calculation.

### 3. CORRECTION PROCESS

The spectral response of the MAPIR camera is shown in Figure 1a, revealing the presence of leakage in some bands. Leakage occurs when a filter designed to block certain wavelengths of light allows some of that light to pass through, leading to inaccurate counts for different bands. The spectral response graph displays the intensity values for each band and indicates that some bands have higher intensity values than expected. The spectral response graph created from the JPG images showed the same amount of leakage as the RAW images, but the ratios were adjusted, either through compression or through an attempt at real-time band correction. However, these adjustments only mask the underlying problem of distortion and do not provide an accurate representation of the spectral response. Integration values obtained from the spectral response graph (see figure 1b) were used to create a 3x3 matrix representing the distortion present in the MAPIR camera.

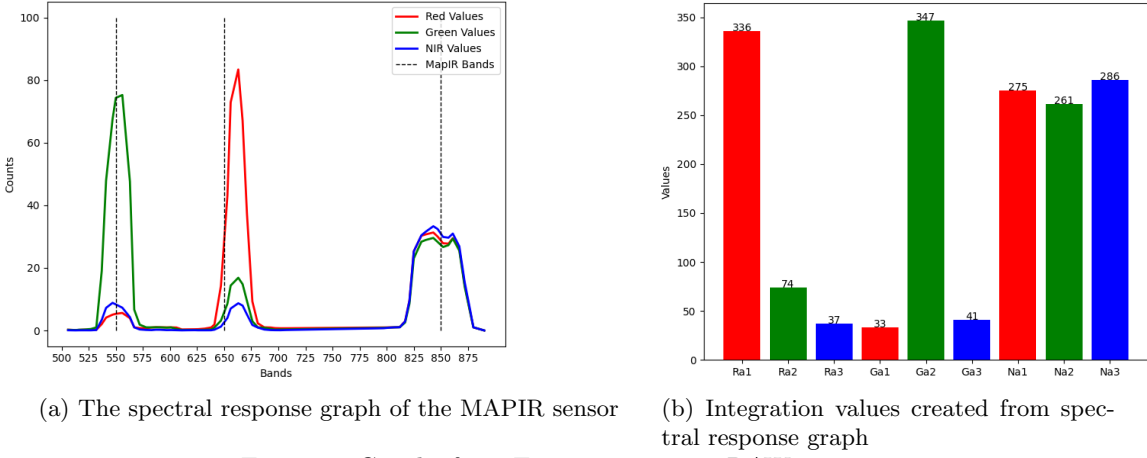


Figure 1: Graphs from Experiment using RAW images

To correct for leakage in the MAPIR camera, the distortion is represented by a 3x3 matrix. Each row of the matrix corresponds to the amount of red, green, and NIR present in each band, while each column represents the RGN bands (see figure 2). Identifying the distortion matrix is essential for creating a correction matrix that can be used to correct the RGN counts detected in a pixel, resulting in an accurate spectral response for the MAPIR camera.

$$Distortion\ Matrix = \begin{bmatrix} a_{11} & a_{12} & a_{13} \\ a_{21} & a_{22} & a_{23} \\ a_{31} & a_{32} & a_{33} \end{bmatrix}$$

Figure 2

A single pixel in the image can be represented by the equation  $p' = d^*p$ , where  $p'$  is the pixel counts matrix detected from the sensor in each band (3x1),  $d$  is the sensor distortion matrix (3x3), and  $p$  is the corrected values matrix (3x1) (see figure 3a). The expanded version of the equation can be represented by  $\begin{bmatrix} [R'] & [G'] & [N'] \end{bmatrix} = [[a_{11}, a_{12}, a_{13}], [a_{21}, a_{22}, a_{23}], [a_{31}, a_{32}, a_{33}]] * [[R], [G], [N]]$  (see figure 3b).

$$p' = dp$$

$$\begin{bmatrix} R' \\ G' \\ N' \end{bmatrix} = \begin{bmatrix} a_{11} & a_{12} & a_{13} \\ a_{21} & a_{22} & a_{23} \\ a_{31} & a_{32} & a_{33} \end{bmatrix} \begin{bmatrix} R \\ G \\ N \end{bmatrix}$$

Figure 3: Pixel equations: simple and expanded

The correction process involves solving for the distortion matrix by setting up the pixel equation using the integration values obtained from the spectral response graph (see figure 1a). An equation for each band needs to be set up to obtain the completed distortion matrix, where p is [1,0,0] for red, [0,1,0] for green, and [0,0,1] for NIR (see figure 4).

$$\begin{bmatrix} 336 \\ 74 \\ 36 \end{bmatrix} = \begin{bmatrix} a_{11} & a_{12} & a_{13} \\ a_{21} & a_{22} & a_{23} \\ a_{31} & a_{32} & a_{33} \end{bmatrix} \begin{bmatrix} 1 \\ 0 \\ 0 \end{bmatrix}$$

(a) Red Band Equation

$$\begin{bmatrix} 33 \\ 347 \\ 41 \end{bmatrix} = \begin{bmatrix} a_{11} & a_{12} & a_{13} \\ a_{21} & a_{22} & a_{23} \\ a_{31} & a_{32} & a_{33} \end{bmatrix} \begin{bmatrix} 0 \\ 1 \\ 0 \end{bmatrix}$$

(b) Green Band Equation

$$\begin{bmatrix} 275 \\ 261 \\ 286 \end{bmatrix} = \begin{bmatrix} a_{11} & a_{12} & a_{13} \\ a_{21} & a_{22} & a_{23} \\ a_{31} & a_{32} & a_{33} \end{bmatrix} \begin{bmatrix} 0 \\ 0 \\ 1 \end{bmatrix}$$

(c) NIR Band Equation

Figure 4: Pixel band equations for distortion matrix

Solving this system of equations yields the completed distortion matrix, as seen in figure 5a. To isolate the [R G N] matrix (p), which represents the corrected values, each side of the pixel equation is multiplied by the inverse of the distortion matrix. The multiplicative inverse of a matrix yields an identity matrix, which is key to the correction process for isolating the correction values for each band. This inversion of the distortion matrix is the correction matrix that will be used to multiply the sensor's detected values (p') to yield the corrected output (see figure 5b).

$$Distortion\ Matrix = \begin{bmatrix} 336 & 33 & 275 \\ 74 & 347 & 261 \\ 37 & 41 & 286 \end{bmatrix}$$

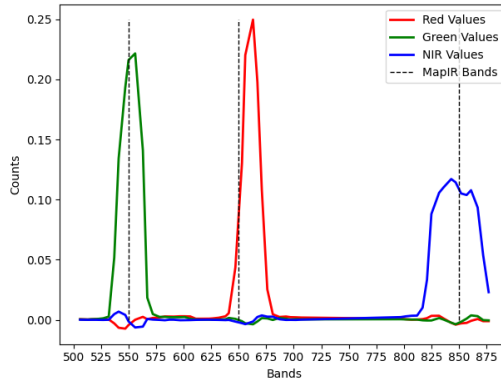
(a) Distortion matrix

$$\begin{bmatrix} R \\ G \\ N \end{bmatrix} = \begin{bmatrix} R' \\ G' \\ N' \end{bmatrix} \begin{bmatrix} 336 & 33 & 275 \\ 74 & 347 & 261 \\ 37 & 41 & 286 \end{bmatrix}^{-1}$$

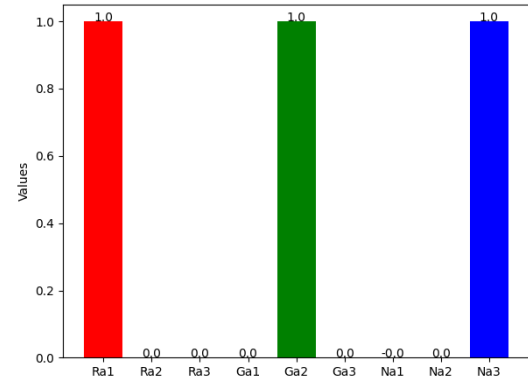
(b) Correction Equation

Figure 5

After correcting all of the images from the monochromator experiment using the correction matrix obtained from the distortion matrix, the resulting spectral response and integration graphs show full isolation of each band (see figure 6). This isolation is crucial for accurate analysis of the images, as it ensures that the counts in each band are not contaminated by leakage from other bands.



(a) The corrected spectral response graph of the MAPIR sen- sor



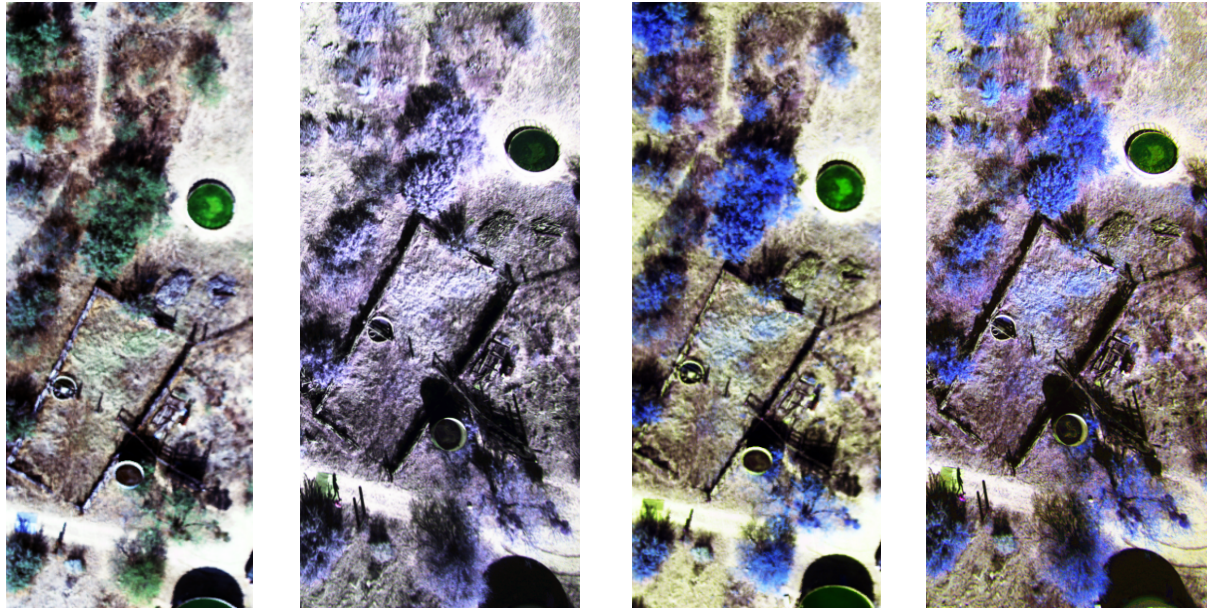
(b) Integration values created from the cor- rected spectral response graph

Figure 6: Graphs from Experiment using corrected images

## 4. RESULTS

In December 2022, the University of Memphis collaborated with the University of Central Florida and the University of Arizona to conduct a field test in Tucson, Arizona. The team captured images of an area that contained vegetation and dead areas at an altitude of approximately 400ft using a Resonon Pika L hyperspectral camera mounted on a custom-built hexacopter drone (see Figure 7a). At a similar altitude, images of the same area were collected using the DJI Mavic Pro Survey3 Bundle<sup>8</sup> purchased from MAPIR, with default camera settings<sup>9</sup> where the NIR band is mapped to the blue channel (see Figure 7b).

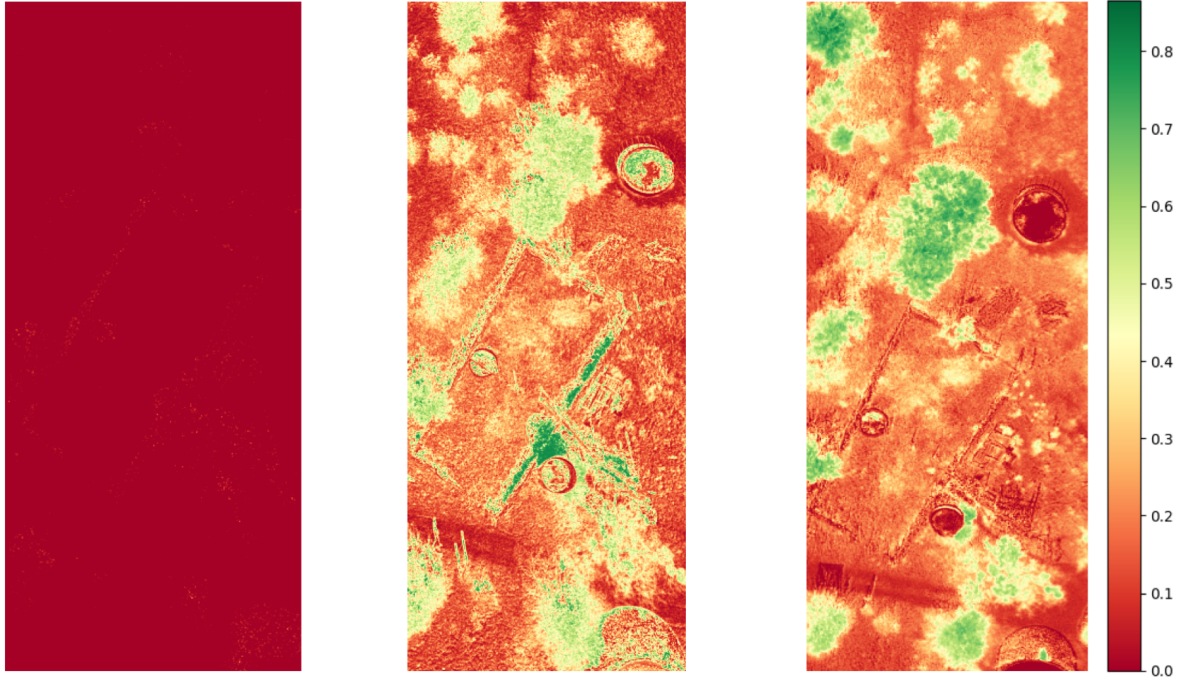
To visually compare the performance of the MAPIR camera with the hyperspectral camera, an RGN rendering from the hyperspectral camera was created and used for comparison with the NIR band mapped to the blue channel.(see Figure 7c). The healthy green vegetation in the image has a significant blue tint, indicating absorption of red light and reflection of NIR light, which is a characteristic of healthy vegetation. Figure 7d shows an RGB rendering of a corrected RAW image from the MAPIR camera. When compared with the RGN image from the hyperspectral camera, the same areas now have a similar blue tint and the images look very similar, indicating that the correction process has effectively improved the MAPIR image to match the spectral characteristics of the hyperspectral image.



(a) RGB rendering from hyperspectral camera for image from MAPIR camera. (b) RGB rendering of RAW image from MAPIR camera for reference. (c) RGN rendering from hyperspectral camera for corrected RAW image from reference. (d) RGB rendering of corrected RAW image from MAPIR camera for MAPIR camera.

Figure 7: Tucson, Arizona scene comparison

RGN cameras can be used to compute various vegetation indices (VI) such as the enhanced vegetation index (EVI), the green normalized difference vegetation index (GNDVI), the soil-adjusted vegetation index (SAVI), and the most popular, the normalized difference vegetation index (NDVI).<sup>10</sup> NDVI is a widely used remote sensing tool that provides information on vegetation health and distribution. It is calculated as the difference between the amount of red and near-infrared light reflected by vegetation, which is related to the amount of chlorophyll in the plant. NDVI values range from -1 to 1, with values closer to 1 indicating healthy vegetation, values closer to 0 indicating sparse or stressed vegetation, and values closer to -1 indicating the absence of vegetation. However, when applying NDVI to an image with leakage present, as shown in Figure 8a, it can result in mostly negative NDVI values, which falsely indicate the absence of vegetation in the area being measured. The corrected NDVI image, as shown in Figure 8b, demonstrates an increase in areas with vegetation and is more consistent with the expected results from applying NDVI to an image. For reference, Figure 8c shows the NDVI from the hyperspectral image.



(a) NDVI from original MAPIR image (b) NDVI from corrected MAPIR image (c) NDVI from hyperspectral image

Figure 8: NDVI Comparison

For a more precise comparison, NDVI measurements of an area were averaged in two separate regions of the image. The first is the interior of the tree right above the paddock fence with a cistern to the right of it and the second is an area inside the paddock fence to the right of the small cistern. Table 1 shows the comparison results for these regions, with values obtained from the hyperspectral image serving as the reference. Our findings suggest that the NDVI values derived from the corrected MAPIR images are similar in both regions, indicating that they can reliably be used for further analysis.

Table 1: NDVI Comparison Table

Region	NDVI MAPIR Raw	NDVI MAPIR Corrected	NDVI Hyperspectral
Tree Area	-0.096	0.573	0.601
Fence Area	-0.175	0.308	0.251

## 5. CONCLUSION

By conducting a series of experiments with the monochromator and hyperspectral camera, we were able to create a correction matrix that could be applied to raw images to improve their accuracy. The process involved identifying and correcting for distortion and leakage present in the camera's spectral response. Our results showed that the correction process effectively improved the MAPIR images to match the spectral characteristics of the hyperspectral images. The corrected images also yielded more accurate NDVI measurements, as demonstrated by the increase in areas with vegetation and the consistency with the expected results from applying NDVI to an image. This highlights the importance of correcting for distortion and leakage in remote sensing tools such as the MAPIR camera when using NDVI to analyze vegetation health and distribution.

## 6. ACKNOWLEDGMENTS

We would like to express our gratitude to everyone who contributed to this research project. First and foremost, we would like to thank our research advisor, Dr. Jacobs, for providing us with guidance and support throughout the project. We would also like to thank the University of Memphis for providing us with the necessary resources and facilities to conduct our research.

We would like to express our appreciation to the University of Central Florida and the University of Arizona for their collaboration on the field test conducted in Tucson, Arizona. We would like to thank MAPIR for providing technical support for the Survey3 Bundle.

We would also like to thank the lab staff for their assistance with equipment setup and calibration, data acquisition, and processing. We would like to acknowledge the funding support from the Center for Applied Earth and Engineering Research (CAESER) and the Department of Defense, which made this research project possible.

## REFERENCES

- [1] Mulla, D. J., "Twenty five years of remote sensing in precision agriculture: Key advances and remaining knowledge gaps," *Biosystems Engineering* **114**(4), 358–371 (2013).
- [2] Jarrell-Ash Company, *Model 82-410 Monochromator: Technical Manual*. Jarrell-Ash Company, 590 LIN-COLN STREET, WALTHAM, MA (1967).
- [3] Resonon, "Resonon pika 1 datasheet," tech. rep., Resonon (2023).
- [4] Klein, A. et al., "imageio v3," (2021).
- [5] Klein, A. et al., "imageio.v3.imread," (2021).
- [6] Malvar, H. S., He, L.-W., and Cutler, R., [High-Quality Linear Interpolation for Demosaicing of Bayer-Patterned Color Images], Microsoft Research (2004).
- [7] Gonzalez, R. C. and Woods, R. E., [Digital Image Processing], Pearson Education, 3 ed. (2009).
- [8] MAPIR, "Dji mavic pro survey3 bundle," (2021).
- [9] MAPIR, *MAPIR Survey3 Camera Manual* (2021).
- [10] Gupta, R., Kondamudi, N., Kharakwal, M. S., and Rai, P. K., "An overview of the methods for calculating vegetation indices, their merits and demerits," *Journal of Remote Sensing & GIS* **6**(4) (2017).